

NUMERICAL SIMULATION OF SHEAR SLITTING PROCESS OF GRAIN ORIENTED SILICON STEEL USING SPH METHOD

Łukasz BOHDAL*, Katarzyna TANDECKA*, Paweł KAŁDUŃSKI*

*Faculty of Mechanical Engineering, Koszalin University of Technology, Raclawicka 15-17 str., 75-620 Koszalin, Poland

lukasz.bohdal@tu.koszalin.pl, katarzyna.tandecka@tu.koszalin.pl, pawel.kaldunski@tu.koszalin.pl

received 5 April 2017, revised 10 December 2017, accepted 12 December 2017

Abstract: Mechanical cutting allows separating of sheet material at low cost and therefore remains the most popular way to produce laminations for electrical machines and transformers. However, recent investigations revealed the deteriorating effect of cutting on the magnetic properties of the material close to the cut edge. The deformations generate elastic stresses in zones adjacent to the area of plastically deformed and strongly affect the magnetic properties. The knowledge about residual stresses is necessary in designing the process. This paper presents the new approach of modeling residual stresses induced in shear slitting of grain oriented electrical steel using mesh-free method. The applications of SPH (Smoothed Particle Hydrodynamics) methodology to the simulation and analysis of 3D shear slitting process is presented. In experimental studies, an advanced vision-based technology based on digital image correlation (DIC) for monitoring the cutting process is used.

Key words: Shear Slitting, Smoothed Particle Hydrodynamics, Grain Oriented Silicon Steel, Digital Image Correlation

1. INTRODUCTION

The process of forming parts from sheet metal using shearing frequently includes blanking, piercing, slitting, and trimming operations. These operations realized with high speed, are a very complicated technological processes in which material undergoes plastic deformations. Grain oriented and non-oriented electrical steels are widely used for the manufacture of transformer cores, power reactors, hydro-generators, turbo-generators and other electrical equipment and apparatuses. Cutting operations for example: blanking, guillotining, edge trimming, shear slitting, or punching induce stresses in electrical steels and consequently magnetic properties are partially deteriorated. According to many authors, the reason for the deterioration of the magnetic properties is to change the distribution of flux density and hysteresis loss (Godec, 1977; Gałęzia et al., 2012; Gontarz and Radkowski, 2012).

The strong deformations are generated in tool-workpiece contact zones which affect on its magnetic properties. The another problem of shearing processes is deterioration of cut surface quality by forming of burrs and rollover which may include increasing the metal core eddy current loss. The burr also strongly difficult the packetizing. The analysis of state of stresses and strain in sheet after shearing using experimental methods is very problematic. This analysis is determined by invasive methods (Eg. by drilling a series of small openings through which wound measuring winding) which increase the error margin and in many cases is impossible when thin sheets are analyzed. There are no known non-invasive methods of appointment.

At the moment knowledge of the slitting of electrical steels is very limited and based mainly on experimental methods, which are often expensive and unable to be extrapolated to other cutting configurations. TeNyenhuis et al., (2000) analyzes the effect of slitting grain-oriented electrical core steel on iron loss which was

investigated by comparing measurements performed by several prominent electrical core steel suppliers with a developed theoretical model. Measurements showed loss increases that were very dependent on sheet width, somewhat dependent on flux density, and practically independent on material type or power frequency. The influence of slitting on core losses and magnetization curve of grain-oriented electrical steel was analyzed by Godec (1977).

Analysis of current literature suggested the main challenge when cutting electrical steels is to obtain high quality products characterized optimum sheared edge condition, minimum surface damage, freedom from burrs, slivers, edge wave, distortion and residual stresses. Simulation of shear slitting processes in which the strip material is highly deformed is a major challenge of FEM codes which number is limited in current literature. The principal problem in using a conventional FE model with Lagrangian mesh are mesh distortion in the high deformation (Golovashchenko, 2006, Kałduński and Kukielka, 2007, 2008, Kukielka et al., 2010). Classical Lagrangian, Eulerian and ALE methods such as finite element methods (FEM) cannot resolve the large distortions very well. Recent developments in so called mesh-free or meshless methods provide alternates for traditional numerical methods in modeling the technological processes (Bagci, 2011; Gałsiorek, 2013; Jianming et al., 2011).

In this paper, first, the applications of mesh-free SPH (Smoothed Particle Hydrodynamics) methodology to the simulation and analysis of 3-D slitting process is presented. This method combines the advantages of mesh-free, Lagrangian, particle methods and eliminate most of difficulties. At the moment in current literature applications of mesh-free methods to modeling of shear slitting and other shearing processes is lacking. Developed model is used to analysis of residual stresses in grain oriented electrical steels during and after process under different conditions. Next, the developed model is validated with experimental research by using vision-based solutions. The effect

of selected process technological parameters on the mechanically affected zone on the workpiece is analyzed.

2. BASIS OF THE SPH METHOD

SPH is total Lagrangian and is a truly mesh-free technique initially developed by Gingold and Monaghan (1977) for the analysis and simulation of astrophysics problems. The idea of this method is to divide a continuum into discrete elements, called particles which are placed at some distance d from each other. This distance is called particle density d (Fig. 1).

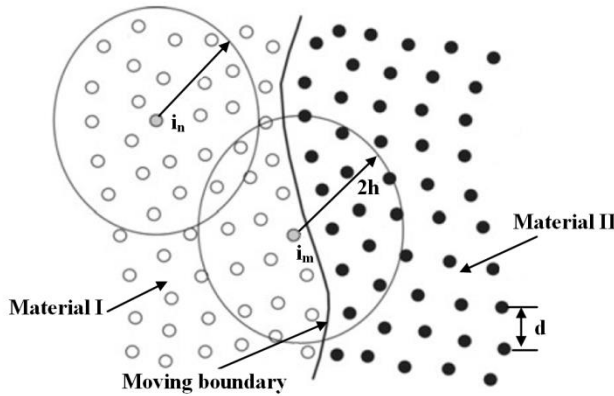


Fig. 1. Smoothing kernel in material volume and at the boundary

The smoothing of field variables is performed in the area with radius h , called the smoothing length, over which the variables are smoothed by a kernel function. This means that the value of a variable in any spatial point can be obtained by adding the relevant values of the variables within two smoothed lengths. Sometimes relative to particle density smoothing length $\bar{h} = h/d$ is used. In contrast to mesh methods such as, e.g., the FEM, in which the mesh distorts in the case of large deformations, the SPH method can be used to model processes accompanied by large deformations. The SPH approximation of the equation for continuum mechanics uses the following approaches. A function $f(x)$ is substituted by its approximation $A_f(x, h)$, characterising a body condition. For example, the velocities of a body's points in a particular area are approximated with the following expression:

$$A_f(x, h) = \int f(y) \cdot W(x, h) dy, \quad (1)$$

where $W(x, h)$ is a smoothed kernel function (Heisel et al., 2013). The size of the smoothing kernel is defined by the function of Θ :

$$W(x, h) = \left(\frac{1}{h(x)^p} \right) \cdot \Theta(x), \quad (2)$$

where p is the dimension of space.

The majority of the smoothing kernels used in the SPH method is represented as cubic B-spline, determining the selection of the function Θ as follows:

$$\Theta(x) = C \cdot \begin{cases} 1 - \frac{3}{2} \cdot x^2 + \frac{3}{4} \cdot x^3, & \text{if } |x| \leq 1 \\ \frac{1}{4} \cdot (2 - x)^3, & \text{if } 1 \leq |x| \leq 2 \\ 0 & \text{if } 2 \leq |x| \end{cases} \quad (3)$$

where C is the normalisation constant. Integration time step can be determined by the following equation:

$$\Delta\tau = C_{\Delta\tau} \cdot \min_i \left(\frac{h_i}{C_i + v_i} \right), \quad (4)$$

where i is the particle number; $C_{\Delta\tau}$ is the time step increase coefficient; v_i is the velocity of particle i . It is important to notice that coefficient $C_{\Delta\tau}$ directly influences the integration time step.

The smoothing length in LS-DYNA solver used in this work dynamically varies so that the number of neighbouring particles remains relatively constant. It is realized by recalculating the smoothing length in accordance with the average particle density:

$$h = h_0 \left(\frac{d_0}{d_i} \right)^{1/p}, \quad (5)$$

or by solving the continuity equation:

$$\frac{dh}{dt} = \frac{1}{d} \cdot \frac{h}{d} \cdot \frac{\partial d}{\partial t}, \quad (6)$$

where d_0 and h_0 are the initial density and the initial smoothing length.

A quadratic approximation of the particle motion is mainly used for the SPH method. A motion of the particles can be described here with the following equation:

$$\frac{\partial v_i^\alpha}{\partial t} = \sum_{j=1}^N m_j \cdot \left(\frac{\sigma_i^{\alpha\beta}}{d_i^2} + \frac{\sigma_j^{\alpha\beta}}{d_j^2} + A_{ij} \right) \cdot \frac{\partial W_{ij}}{\partial x_i^\beta}, \quad (7)$$

where j is particle number; N is the number of neighbouring particles; $v_i^\alpha = \frac{dx_i^\alpha}{dt}$ is the velocity of particle i ; m_j is the mass of particle j ; $\sigma_i^{\alpha\beta}$, $\sigma_j^{\alpha\beta}$ are the stress tensors of i and j particles respectively; d_i and d_j are the densities of i and j particles respectively; A_{ij} are the specific external forces; $W_{ij} = W(x_i - x_j, h)$ is the smoothing kernel.

3. CONSTITUTIVE MODEL FOR MATERIAL

In slitting models, accurate and reliable flow stress models are considered as highly necessary to represent workpiece materials constitutive behavior. The constitutive material model reported by Johnson and Cook (1985) was employed in this study, it is often used for ductile materials in cases where strain rate vary over a large range and where adiabatic temperature increase due to plastic heating cause material softening. The model can be represented by Eq (8):

$$\sigma_Y = [A + B(\bar{\epsilon}^p)^n][1 + C \ln \dot{\epsilon}^*][1 - (T^*)^m], \quad (8)$$

where σ_Y is the equivalent flow stress, $\bar{\epsilon}^p$ is the equivalent plastic strain, A , B , and n are strain hardening constants; C is the strain rate hardening constant, and m is the thermal softening constant that modifies the homologous temperature term, T^* . The homologous temperature is defined as, $T^* = \frac{T - T_r}{T_m - T_r}$, where T is the temperature of the material, T_r is a reference temperature (typically room temperature), and T_m is the melt temperature of the material. The term, $\dot{\epsilon}^*$, is the normalized strain rate of the material or $\dot{\epsilon}^* = \frac{\dot{\epsilon}^p}{\dot{\epsilon}_0}$, where $\dot{\epsilon}_0 = 1.0s^{-1}$. A dilatation of the material is based on the value of equivalent plastic strain at element integration points. Failure occurs when $D = 1$. The damage parameter follows a cumulative damage law given by Eq (9):

$$D = \sum \frac{\Delta \bar{\epsilon}^P}{\epsilon_f}, \quad (9)$$

where $\Delta \bar{\epsilon}^P$ is the increment of the equivalent plastic strain during an integration cycle and ϵ_f the equivalent strain to fracture under current conditions of strain rate, temperature, pressure and equivalent stress (Bohdal et al., 2015, Gontarz and Radkowski, 2012, Heisel et al., 2013). ET 122-30 (0,3 mm thick) grain oriented steel which is often employed for industry, is used to simulate typical production conditions. The mechanical and physical properties of material are shown in Tab. 1. The Johnson-Cook constitutive model constants are shown in Tab. 2.

Tab. 1. Mechanical and physical properties of work material (Bohdal et al., 2015)

Density [kg/dm ³]	Silicon content [%]	Yield point [MPa]	Tensile strength [MPa]	Elongation [%]	Hardness [HV ₅]
7.65	3.1	300	370	11	160

Tab. 2. The Johnson-Cook constitutive model constants for ET 122-30 steel (Bohdal et al., 2015)

A [MPa]	B [MPa]	C	N	M
104.3	445.6	0.041	0.46	0.54

4. SPH MODEL OF SHEAR SLITTING PROCESS

Slitting differs from the other shearing operations such as blanking and punching as it involves the rotation of blades and hence the material is cut in two directions simultaneously instead of one. A thorough understanding of the process of slitting would thus require that a three-dimensional analysis of the process be conducted. A three-dimensional SPH model of slitting was developed in the general purpose finite element software package LS-DYNA and presented in Fig. 2a. The model is created based on the experimental configuration and the geometrical parameters of the test stand shown in Fig. 2b. For the monitoring of slitting process, a high-speed camera i-SPEED TR with zoom lens and light sources are used.

The slitting machine (KSE 10/10) consists of two rotary knives (where: $r_1 = r_2 = 15$ mm, $r_3 = 20$ mm) driven by the engine. The contact between the knives and sheet (where: $l = 80$ mm, $w_i = 40$ mm) is considered non-sliding contact that uses a polyurethane roll, which move the sheet in the horizontal direction. The kinematics of the different components is as follows: first the upper knife moves vertically with the constant velocity v_1 in order to cut the sheet thickness. Then, the sheet moves along Z axis with the constant velocity $v_2 = 3$ m/min as a result of knives and roll rotations. In order to reduce the model size and shorten the computational time the strip is modeled by SPH particles while the tools (knives) are considered as rigid bodies, and modeled by the traditional finite element method. The contact between tools and the deformable sheet metal is described using Coulomb's friction model, and constant coefficients of static friction $\mu_s = 0.08$ and kinetic friction $\mu_d = 0.009$ are accepted.

A series of numerical simulations are carried out to determine the optimal parameters of the solver, and to obtain a minimum prediction error of slitting variables and minimal simulation cost. The computer simulations are executed for different initial particle

densities: $d_1 = 0.025$ mm, $d_2 = 0.02$ mm, $d_3 = 0.016$ mm, $d_4 = 0.014$ mm, $d_5 = 0.0125$ mm. As a simplifying assumption the flat state of the deformation is assumed (Fig 3).

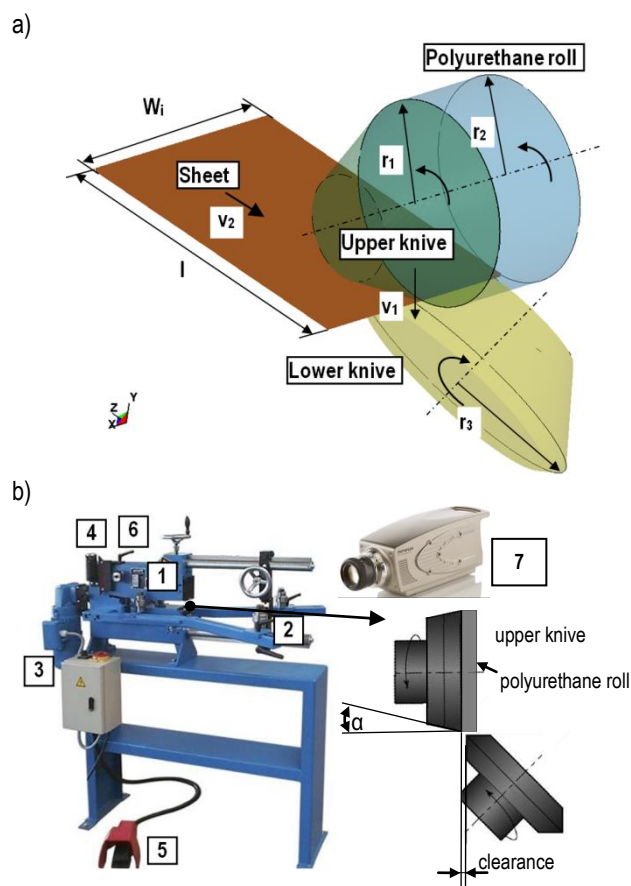


Fig. 2. a) SPH simulation model of shear slitting process, b) experimental test stand: 1 – knives, 2 – sheet holder, 3 – engine, 4 – clearance regulator, 5 – drive pedal, 6 – slitting velocity regulator, 7 – high-speed camera

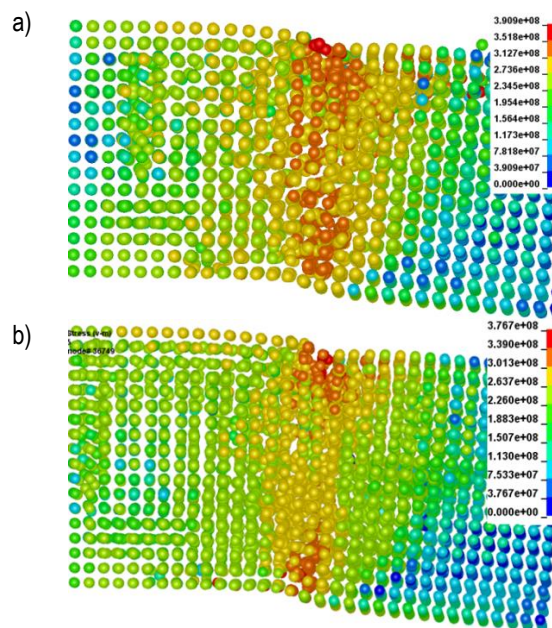


Fig. 3. Stress intensity distribution in plastic flow phase of the process for different initial particle density: a) $d_2 = 0.02$ mm, b) $d_3 = 0.016$ mm

An initial particle density of $d_4 = 0.014$ mm is selected as an optimal SPH particle density for used model dimensions. This initial particle density is selected so as to have a reasonable number of particles at the thickness of the sheet (Fig. 3). Larger density does not illustrate the material flow features and stress distributions appropriately because the material consists of many empty spaces between particles (Fig. 3a). Smaller initial particle density strongly increases the computing time. Stabilization of the stress distribution, its values and slitting force in each time step is reached when $d \leq 0.014$ mm.

From our previous researches it's clear that changing the values of smoothing length between $h = 1.05 \div 1.3$ (recommended by solver options) has a small influence on stress distribution, its values and deformation state (Bohdal, 2016). Higher values of smoothing length strongly increase the simulation time, without significant effect on maximum stress variables and deformation state during process. For presented analyses in this paper a value of $h = 1.2$ is used.

5. SIMULATION RESULTS

5.1. Analysis of slitting mechanism

Proposed method using advanced vision based system allows for analysis of states of deformations in cutting area, propagation of cracking and analysis of its trajectory. An analysis of areas of high displacements and strains taking into account geometrical and physical nonlinearities of the process is possible.

Example results are given at Figs. 4 – 7.

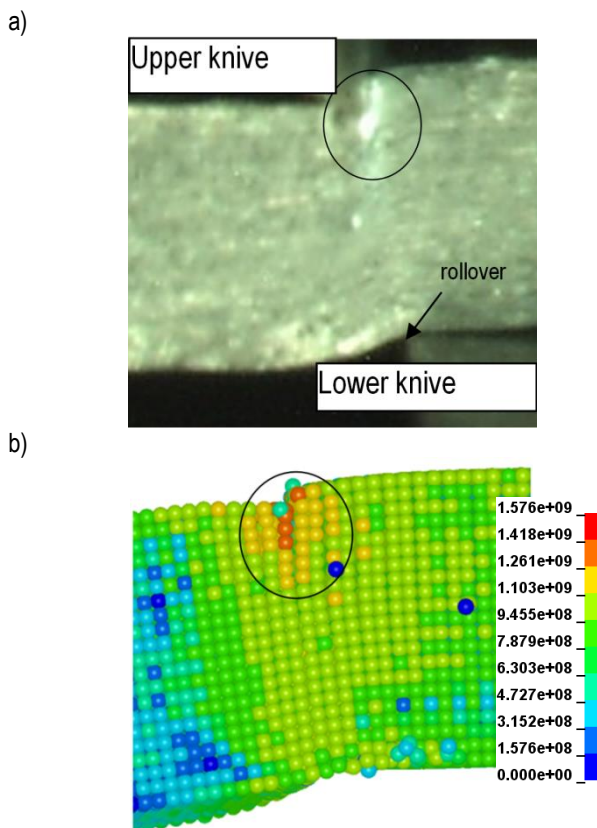


Fig. 4. Elastoplastic phase of the slitting process: a) image from camera, b) SPH simulation (equivalent stress distribution)

During the slitting process four main phases can be observed: elastic, elastoplastic, elastoplastic in which damage occurs, initiation and propagation of cracks leading to final rupture. During the first part of the process at crack front area, the upper and lower knives indent the sheet, pulling down some surface material. The greatest deformation of material occurs near the cutting edges of the tools in this phase (Fig. 4). First step of formation of rollover can be observed.

During the second phase the intensive plastic flow of the material in the surroundings of the cutting surface can be observed (Fig. 5a). A characteristic distortion of SPH particles in this areas can be seen (Fig. 5b). Both in numerical model and experimental investigations the plastic strain localization zones propagate much faster from the lower knife blade than from the upper knife (Figs. 5a, b). The deformation zone is non-symmetric with respect to the top and bottom knives. It can be observed the large distortions of the SPH particles near the bottom edge of sheet just before burr formation (Fig. 5b). The mechanically affected zone in this area is extended along the x direction. Since the crack will initiate and propagate through the localization zone, the cut surface will be curved and the burr will form because the crack will not run to the bottom blade tip (Fig. 5c). Comparison of the characteristic features of material separation geometry obtained from numerical model and experiment shows good agreement in the length of burnished and rollover areas (Fig. 5c). Some differences occur in the measurement of the fracture area, because in the SPH model moment of separation of material is delayed.

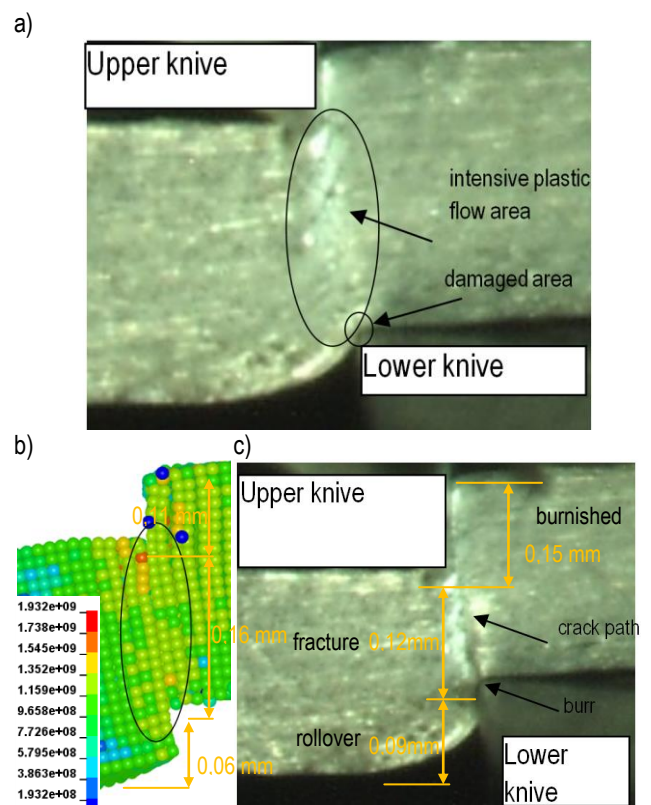


Fig. 5. Elastoplastic phase in which damage occurs: a) image from camera, b) SPH simulation (equivalent stress distribution), c) image from camera with visible initiation and propagation of cracks

As the sheet slits, it moves tangentially to the blade (Fig. 6). This causes the area of contact with the knife blade on the sheet to be inclined to the horizontal at an angle. It can be seen that the stresses form some bending moments. The sheet is bent twice to conform to the shape of the knives (Fig. 6a). The highest equivalent stress appears in the primary deformation zone, and a large plastic deformation also exists around this zone. A characteristic shear stress distribution extended along the x direction is observed under the upper knife edge (Figs. 6a and b). At the final stage of the process the tool - sheet contact zone is reduced (Fig. 6c). The bending moment increases which may cause rupture of the material at the end of the shearing line and burr formation.

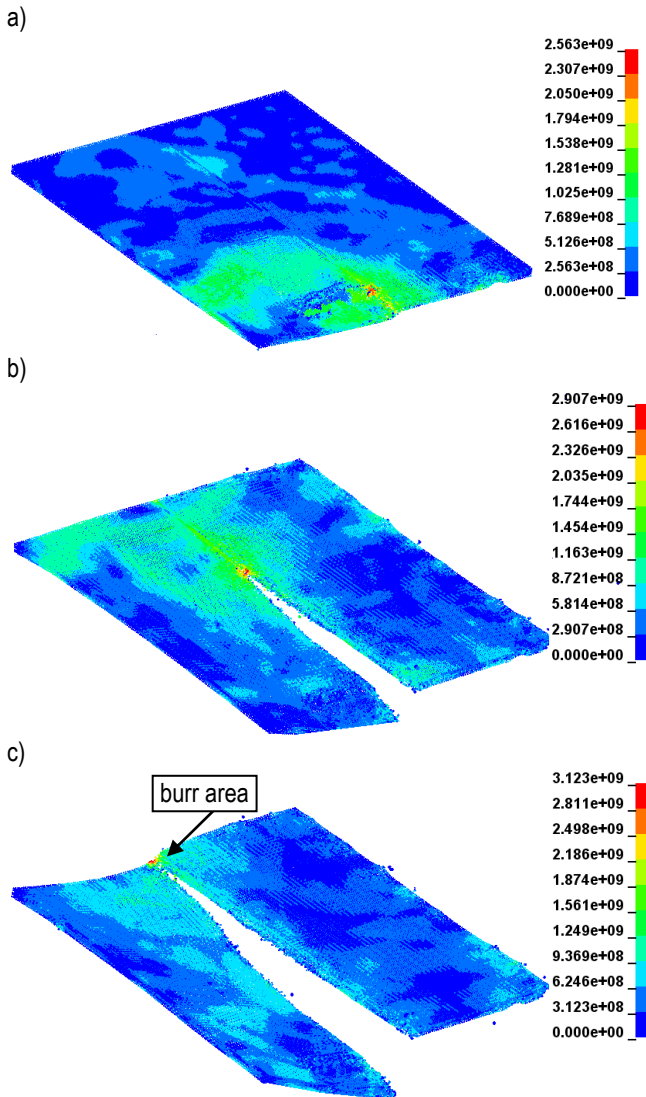


Fig. 6. Equivalent stress distribution in various stages of process: a) 5% step time, b) 60% step time, c) 95% step time

5.2. Parametric study

In this section, we illustrate the present solution procedure's capability to reproduce the effects of chosen process technological parameters such as the rake angle of the upper knife α , and clearance h_c on the mechanically affected zone on workpiece. According to works (Meehan and Burns, 1996; TeNyenhuis et al., 2000; Pluta et al., 2004; Chodor and Kukielka, 2007; Chodor and Kukielka, 2014; Kulakowska et al., 2014) the deformation-affected

zone after cutting process extends to several millimeters away from the cut edge and possibly occupies the entire sample volume. Thus, understanding the local degradation of the material due to the cutting process is crucial for improving the fabrication process and also for the design and simulation of electrical machines.

The computer simulations and experiments are executed for different rake angle values of $\alpha = 5 \div 40^\circ$, and clearance values of $h_c = 0.02 \div 0.1$ mm. Figure 7 shows the influence of analyzed process parameters on the extend of deformation affected zone. As the horizontal clearance increases, the deformation affected zone increases. The maximum width of deformation affected zone was found using a horizontal clearance of $h_c = 0.1$ mm. Reducing the clearance to $h_c = 0.02$ mm significantly reduced the affected zone for used rake angles. Unfavourable deformation conditions occur when the rake angle is set to the middle range (20 - 25°). The width of deformation affected zone carry out then approximately 170 - 190 μm . Increasing the rake angle from $\alpha = 25^\circ$ to $\alpha = 40^\circ$ significantly reduces this area at the analysed velocities and vertical clearances.

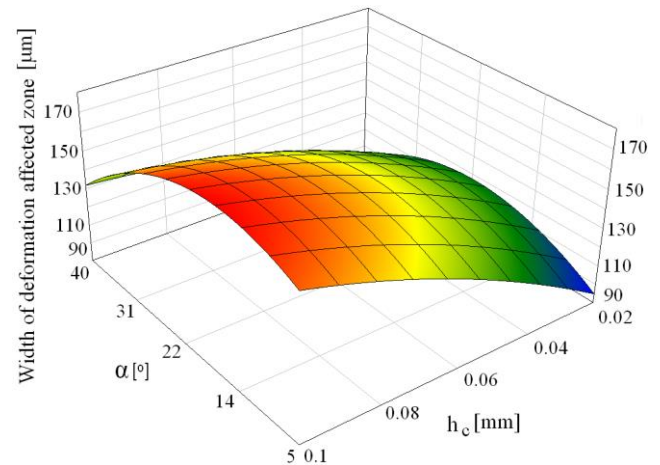


Fig. 7. Influence of rake angle α and clearance h_c on the width of deformation affected zone

6. CONCLUSIONS

The paper presents a possibility to apply the mesh-free SPH method for the analysis of the shear slitting operation. The objective of this study was to develop a three-dimensional model of the slitting process of grain oriented electrical steel. This model should provide insight into this process, which can be used to improve the quality and productivity of slitting. Obtained results showed a significant effect of selected process parameters on the residual stresses and width of deformation affected zone on workpiece. Knowledge about residuals stresses and deformation zone is very important in designing process. The good agreement between simulation results and the experimental data have confirmed the correctness and credibility of the model. Actual investigations concern the analysis of slitting parameters both on residual stress fields and magnetic properties of electrical steels. In modeling using SPH further work is still to be done in order to introduce some other effects concerning the behavior of the rolled metal sheets as the damage induced anisotropy and the spring-back effects.

REFERENCES

1. **Bagci E.** (2011), 3-D numerical analysis of orthogonal cutting process via mesh-free method, *International Journal of Physical Sciences*, 6, 1267-1282.
2. **Bohdal L.** (2016), The application of the smoothed particle hydrodynamics (SPH) method to the simulation and analysis of blanking process, *Mechanika*, 22(5), 380-387.
3. **Bohdal Ł., Gontarz S., Kukielka L., Radkowski S.** (2015), Modeling of residual stresses induced in shear slitting of grain oriented silicon steel using SPH method, *Intelligent Methods in Surface Forming*. Gorzów Wlkp. – Poznań, 13-25 (In Polish).
4. **Chodor J., Kukielka L.** (2007), Numerical analysis of chip formation during machining for different value of failure strain, *PAMM* 7 (1), 4030031-4030032.
5. **Chodor J., Kukielka L.** (2014), Using nonlinear contact mechanics in process of tool edge movement on deformable body to analysis of cutting and sliding burnishing processes, *Applied Mechanics and Materials*, 474, 339-344.
6. **Gałęzia A., Gontarz S., Jasiński M., Mączak J., Radkowski S., Seńko J.** (2012), Distributed system for monitoring of the large scale infrastructure structures based on analysis of changes of its static and dynamic properties, *Key Engineering Materials*, 518, 106-118.
7. **Gąsiorek D.** (2013), The application of the smoothed particle hydrodynamics (SPH) method and the experimental verification of cutting of sheet metal bundles using a guillotine, *Journal of Theoretical and Applied Mechanics*, 51(4), 1053-1065.
8. **Gingold RA., Monaghan JJ.** (1977), Smooth particle hydrodynamics: theory and application to non-spherical stars, *Monthly Notices of the Royal Astronomical Society*, 181, 375-389.
9. **Godec Z.** (1977), Influence of Slitting on Core Losses and Magnetization Curve of Grain Oriented Electrical Steels, *IEEE Trans. Magn.*, 13 (4), 1053-1057.
10. **Golovashchenko S.F.** (2006), A study on trimming of aluminum autobody sheet and development of a new robust process eliminating burrs and slivers, *International Journal of Mechanical Sciences*, 48, 1384-1400.
11. **Gontarz S., Radkowski S.** (2012), Impact of various factors on relationships between stress and eigen magnetic field in a steel specimen. Magnetics, *IEEE Transactions on*, 48 (3), 1143-1154.
12. **Heisel U., Zaloga W., Krivoruchko D., Storchak M., Goloborodko L.** (2013), Modelling of orthogonal cutting processes with the method of smoothed particle hydrodynamics, *Production Engineering Research and Development*, 7, 639-645.
13. **Jianming W., Feihong L., Feng Y., Gang Z.** (2011), Shot peening simulation based on SPH method, *International Journal of Advanced Manufacturing Technology*, 56, 571-578.
14. **Johnson G.R., Cook W.H.** (1985), Fracture characteristics of three metals subjected to various strains, strain rates, temperatures and pressures, *Engineering Fracture Mechanics*, 21(1), 31-48.
15. **Kalduński P., Kukielka L.** (2007), The numerical analysis of the influence of the blankholder force and the friction coefficient on the value of the drawing force, *PAMM* 7 (1), 4010045-4010046.
16. **Kalduński P., Kukielka L.** (2008), The sensitivity analysis of the drawpiece response on the finite element shape parameter, *PAMM* 8 (1), 10725-10726.
17. **Kukielka L., Kulakowska A., Patyk R.** (2010), Numerical modeling and simulation of the movable contact tool-workpiece and application in technological processes, *Journal of Systemics, Cybernetics and Informatics*, 8/3, 36-41.
18. **Kulakowska A., Patyk R., Bohdal Ł.** (2014), Application of burnishing process in creating environmental product, *Annual Set The Environment Protection*, 16, 323-335 (In Polish).
19. **Meehan R. R., Burns S. J.** (1996), Mechanics of slitting and cutting webs, *Experimental Mechanics* 38, 103-109.
20. **Pluta W., Kitz E., Krismanic G., Rygal R., Soinski M., Pfützner H.** (2004), Rotational power loss measurement of Fe based soft magnetic materials; *Poster: 2DM 1&2 Dimensional Magnetic Measurement and Testing*, Ghent University; 27.09.2004 - 28.09.2004; in: 8th International Workshop on 1&2 Dimensional Magnetic Measurement and Testing, S. 9.E.
21. **TeNyenhuis E., Girgis R.** (2000), Effect of slitting electrical core steel on measured iron loss. *Journal of Magnetism and Magnetic Materials*, 215-216, 110-111.